Article

A Ratiometric Two-Photon Fluorescent Probe Reveals Reduction in Mitochondrial H2S Production in a Parkinson's Disease Gene Knockout Astrocytes

Sung Keun Bae, Cheol Ho Heo, Dong Joo Choi, Debabrata Sen, Eun-Hye Joe, Bong Rae Cho, and Hwan Myung Kim

J. Am. Chem. Soc., **Just Accepted Manuscript** • DOI: 10.1021/ja404004v • Publication Date (Web): 07 Jun 2013

A Ratiometric Two-Photon Fluorescent Probe Reveals Reduction in Mitochondrial H_2S Production in a Parkinson's Disease Gene Knockout Astrocytes

Sung Keun Bae,[‡a] Cheol Ho Heo,[‡a] Dong Joo Choi,[‡b] Debabrata Sen,[a] Eun-Hye Joe,[b] Bong Rae Cho,*[c] and Hwan Myung Kim*[a]*

[a]Division of Energy Systems Research, Ajou University, Suwon 443-749, Korea

[b]Department of Pharmacology/Neuroscience Graduate Program, Ajou University School of Medicine, Suwon 443-721, Korea

[c]Department of Chemistry, Korea University, Seoul 136-701, Korea

RECEIVED DATE (to be automatically inserted after your manuscript is accepted if required according to the journal that you are submitting your paper to)

ABSTRACT

Hydrogen sulfide (H_2S) is a multifunctional signaling molecule that exerts neuroprotective effects in oxidative stress. In this article, we report a mitochondria-localized two-photon probe (SHS-M2) that can be excited by 750 nm femtosecond pulses and ratiometrically detect H_2S in live astrocytes and living brain slices using two-photon microscopy (TPM). SHS-M2 showed a bright two-photon excited fluorescence and a marked blue-to-yellow emission color change in response to H_2S, low cytotoxicity with easy loading and minimum interference from other biologically relevant species including reactive sulfur, oxygen and nitrogen species, thereby allowing quantitative analysis of H_2S level. Molecular TPM imaging with SHS-M2 in astrocytes reveals that there is a correlation between the ratiometric analysis and expression levels of cystathionine β-synthase (CBS), the major enzyme that catalyzes H_2S production. In comparison to wild-type controls, the attenuated H_2S production was observed in DJ-1 (a Parkinson's disease gene) knockout astrocytes and brain slices where CBS expression is decreased. These findings demonstrate that reduced H_2S levels in astrocytes may contribute to the development of Parkinson's disease (PD), and SHS-M2 may be useful as a marker to detect a risk of neurodegenerative diseases including PD.

KEYWORDS. Hydrogen sulfide · fluorescent probe · mitochondria · Parkinson's disease · two-photon microscopy.

Introduction

Hydrogen sulfide (H_2S) is an endogenous signalling molecule produced by enzymes such as cystathionine β-synthase (CBS), cystathionine γ-lyase (CSE) and 3-mercaptopyruvate sulfurtransferase (3MST).[1] H_2S has diverse functions in several pathophysiological processes such as neurotransmittion, modulation of redox status, neuroprotection from oxidative stress, and anti-inflammation.[2-4] Mitochondrial H_2S has been recognized to exert protective effects in oxidative stress leading to the

dysfunction and cell death.[5-7] In the brain, there is relatively high concentration of H_2S while CBS has been identified as the major H_2S producing enzyme, which is mainly expressed in astrocytes.[8-11] Defects in H_2S production in the brain could be related to neurodegenerative diseases. Moreover, H_2S treatment protects neurons in Parkinson's disease (PD) animal models.[10,12]

In order to understand its biological and pathological roles, it is crucial to monitor mitochondrial H_2S in live cells and tissues in normal and abnormal systems. To detect H_2S in cells, a number of fluorescent probes derived from azide,[13] azamacrocyclic copper(II) ion complex,[14] and H_2S-specific Michael acceptors[15] have been reported. However, most of them have limitations imposed by fluorescent turn-on responses at single detection window and/or their short excitation wavelength encountered by most conventional probe. The turn-on response can vary depending on the experimental conditions such as incident laser power and/or probe distribution, thereby a quantitative measurement of H_2S was not possible. More recently, a mitochondrial-targeted ratiometric fluorescent probe for H_2S has been also reported.[16] However, the short excitation wavelength limits their application in live tissue imaging due to the shallow penetration depth.

An attractive approach to the detection of H_2S in live cells and tissues is ratiometric imaging with two-photon microscopy (TPM). TPM, which employs two near-infrared photons as the excitation source, offers a number of advantages including greater penetration depth (> 500 μm), localization of excitation, and longer observation times.[17-19] Therefore, there is a strong need to develop a ratiometric TP probe for mitochondrial H_2S.

In this work, we developed ratiometric TP probes (SHS-M1 and SHS-M2, Scheme 1) for mitochondrial H_2S, derived from 6-(benzo[*d*]thiazol-2'-yl)-2-(*N*,*N*-dimethylamino)naphthalene as the fluorophore, 4-azidobenzyl carbamate as the H_2S response site,[13a] and triphenylphosphonium salt (TPP) as the mitochondrial targeting moiety (Scheme 1).[20] We anticipated that thiolate-triggered reaction with azide would cleave the carbamate linkage and liberate the amino group, thereby shifting the emission maxima and increasing the TP cross section.[21]

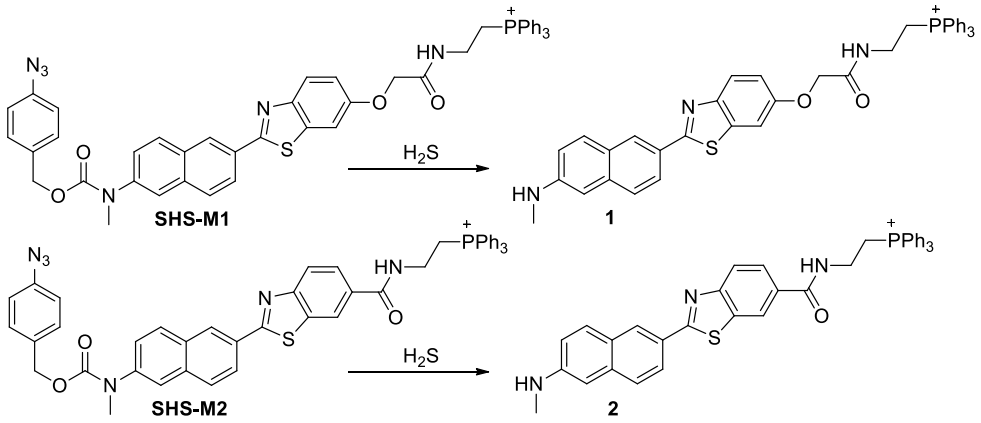

Scheme 1. Structures of SHS-M1, SHS-M2, **1** and **2**.

Results and Discussion

Spectroscopic properties of SHS-M1 and SHS-M2

The preparation of SHS-M1 and SHS-M2 is described in the Supporting Information. The solubilities of SHS-M1 and SHS-M2 in HEPES buffer (30 mM HEPES, 100 mM KCl, pH 7.4) are approximately 3–5 μM, which is sufficient to stain the cells (Figure S1, SI). Under this condition, SHS-M1 and **1** exhibit absorption maxima (λ_{abs}) at 340 nm ($\varepsilon = 1.90 \times 10^4$ $M^{-1}cm^{-1}$) and 365 nm ($\varepsilon = 1.80 \times 10^4$ $M^{-1}cm^{-1}$), with emission maxima (λ_{fl}) at 420 nm ($\Phi = 0.23$) and 500 nm ($\Phi = 0.50$), respectively (Table 1). The λ_{abs} of SHS-M1 and SHS-M2 are nearly the same, while that of **2** is red-shifted from **1** by 18 nm (Figure 1 and Table 1), presumably because of the stronger electron-withdrawing group. The larger Stokes shifts observed for SHS-M2 and **2** compared to SHS-M1 and **1** can also be attributed to the greater stabilization of the charge-transfer excited state in the former that contains a stronger electron-withdrawing group. Consistently, the emission spectra of **1** and **2** showed larger red-shifts with the solvent polarity than those of SHS-M1 and SHS-M2 ($\Delta\lambda_{fl}$ = 16–45 vs 56–72 nm, Figure S2 and Table S1, SI). Further, the two-photon excited fluorescence (TPEF) spectra of **1** and **2** measured in HeLa cells were similar to those measured in EtOH (Figure S2b,d), indicating that EtOH can adequately represent the polarity of the cellular environments.

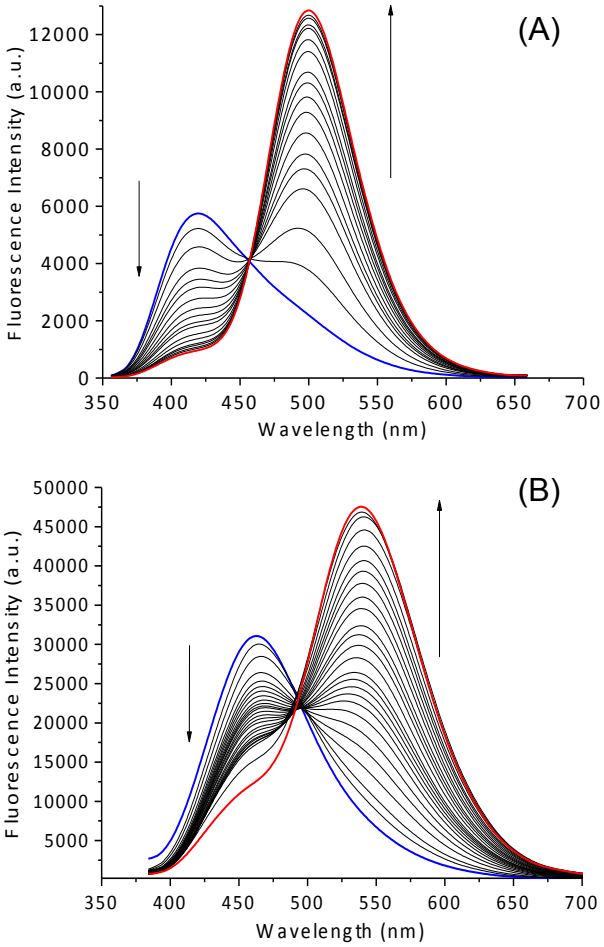

Figure 1. Fluorescence response with time for the reactions of 1 μM (A) SHS-M1 and (B) SHS-M2 with 100 μM Na_2S in the HEPES buffer (30 mM HEPES, 100 mM KCl, pH 7.4). Spectra were acquired at 0 to 60 min after addition of Na_2S. The λ_{ex} = 340 nm (A) and 373 nm (B).

The reaction between SHS-M1 (or SHS-M2) and Na_2S (a commonly employed H_2S donor)[14,15,22] produced **1** (or **2**) as the only major product as monitered by fluorescent emission (Figure 1) and LC-MS analysis (Figure S3, SI). The emission spectra of a 1 μM solution of SHS-M1 treated with 100 μM Na_2S in HEPES buffer increased gradually at 500 nm with a concomitant decrease at 420 nm (Figure 1a). A similar result was observed for SHS-M2, except that both λ_{fl} were significantly red-shifted (Figure 1b). These processes followed pseudo 1st-order kinetics with k_{obs} = 1.4 × 10^{-3} s^{-1} and 9.1 × 10^{-4} s^{-1} for SHS-M1 and SHS-M2, respectively (Figure S4). Moreover, the plots of k_{obs} versus [Na_2S] are straight lines

passing through the origin (Figure S4, SI), indicating that the reactions are overall 2nd order with k_2 = 5.8 $M^{-1}s^{-1}$ and k_2 = 7.0 $M^{-1}s^{-1}$ for SHS-M1 and SHS-M2, respectively. These results can be attributed to the rate-limiting attack of the thiolate ion at azide group followed by the cleavage of the carbamate moeity to afford **1** or **2**, as reported.[21] Further, the *in vitro* detection limits of H_2S with SHS-M1 and SHS-M2 are 0.2 and 0.4 μM (Figure S5), respectively.

SHS-M1 and SHS-M2 showed good selectivity for Na_2S over other biologically relevant reactive sulfur (RSS), oxygen (ROS) and nitrogen species (RNS) (Figure 2). Both probes displayed ~5−8-fold greater response for H_2S over 10 mM glutathione (GSH, 100-fold larger amount than H_2S tested), 1 mM cysteine (Cys), and 1 mM 2-mercaptoethanol (2-ME). Moreover, these probes displayed strong response upon addition of 100 μM Na_2S in the presence of GSH (10 mM) or Cys (1 mM) (Figure 2), thereby conforming the high selectivity for H_2S over GSH and Cys. Other biologically relevant RSS (lipoic acid, SO_3^{2-}, $S_2O_3^{2-}$, SCN^-), RNS (NO_2^-, NO), ROS (H_2O_2, O_2^-, *t*-BuOOH, HOCl), amino acids without thiol groups (ala, glu), and metal ions (Ca^{2+}, K^+, Na^+, Fe^{3+}, Zn^{2+}, Mg^{2+}) showed negligible responses (Figure 2). Further, SHS-M1 and SHS-M2 were pH insensitive at a biologically relevant pH range (Figure S6, SI). Therefore, these probes can detect the intracellular sulphide with minimum interference from other biologically relevant analytes and pH.

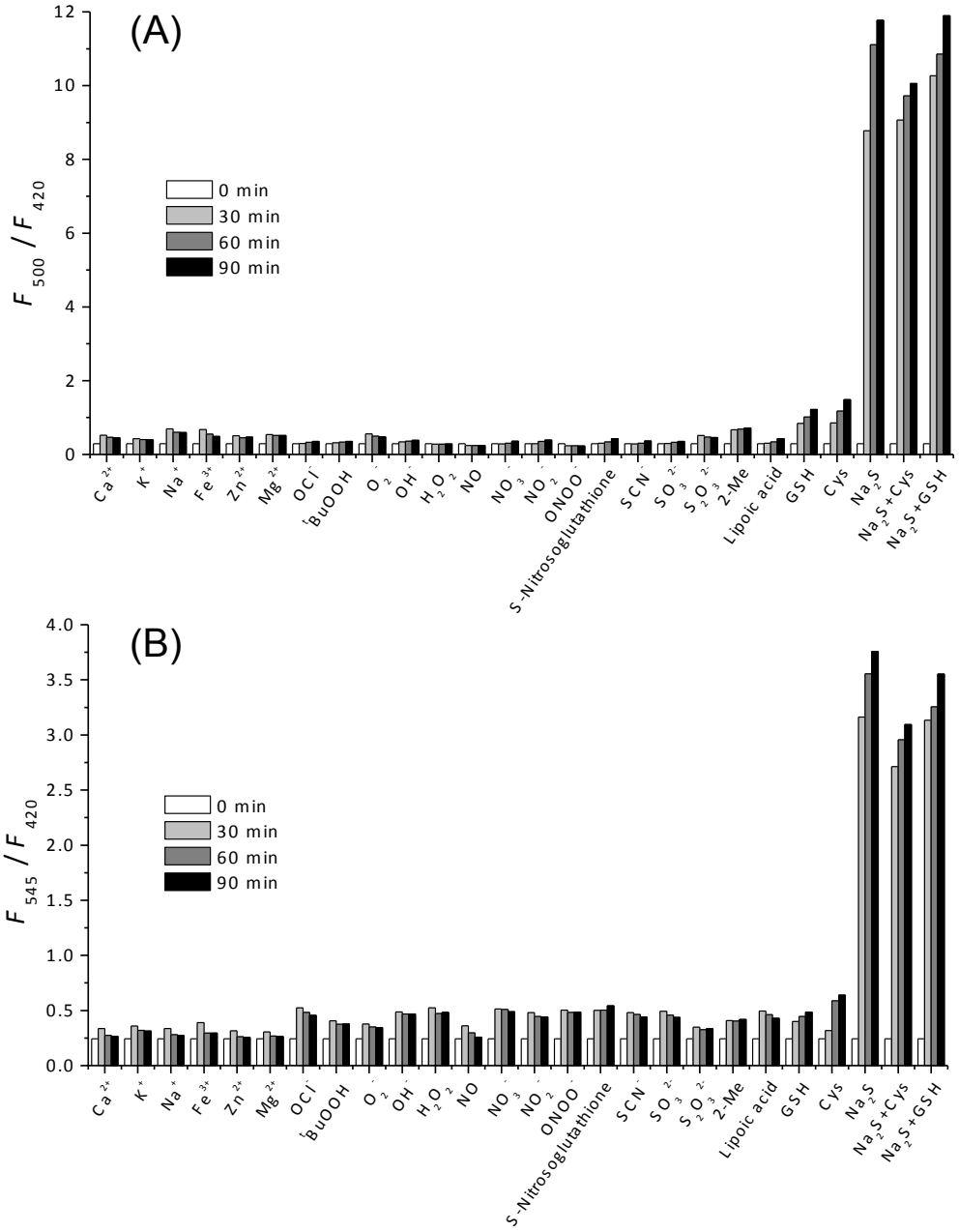

Figure 2. Fluorescence responses of 1 μM (A) SHS-M1 and (B) SHS-M2 toward 100 μM Na_2S, and other reactive sulfur, nitrogen, and oxygen species, as well as amino acids and metal ions. Bars represent the ratio of the emission intensities at λ_{fl} at 0, 30, 60 and 90 min after addition of RSS, RNS, ROS, amino acids, or metal ions. Data were acquired in HEPES buffer (pH 7.4). The λ_{ex} = 340 nm (A) and 373 nm (B).

The TP action cross sections ($\Phi\delta_{max}$) were determined by investigating the TPEF spectra with rhodamine-6G as the reference (SI).[23] The $\Phi\delta_{max}$ values of SHS-M1, **1**, SHS-M2, and **2** are 14, 63, 17, and 55 GM, respectively (Table 1 and Figure S7, SI). The larger values of **1** and **2** than those of SHS-

M1 and SHS-M2 can be attributed to the enhanced donor or acceptor abilities, respectively[24] (Table 1). In EtOH, which is a good model for the cellular environment (*vide supra*), the $\Phi\delta_{max}$ of SHS-M2 and **2** is 1.9−2.3-fold larger than those of SHS-M1 and **1**. Indeed, the TPM images of the cells labeled with SHS-M2 are much brighter than those labeled with SHS-M1, while both probes show high photostability (Figure S8, SI). Moreover, the emission spectra of SHS-M2 in EtOH increased gradually at 510 nm with a concomitant decrease at 445 nm in the presence of excess Na_2S with $k_2 = 4.6\ M^{-1}s^{-1}$, a result similar to that observed in HEPES buffer (Figure S9, SI). The relative emission intensity ratios (F_{yellow}/F_{blue}) at 425-470 nm (F_{blue}) and 525-575 nm (F_{yellow}) showed a 9-fold increase, establishing that SHS-M2 can serve as a ratiometric fluorescent probe for H_2S in cells. Therefore, we have used SHS-M2 in the imaging experiments.

Table 1. Photophysical data for SHS-M1, SHS-M2, **1**, and **2**.

Cpd[a]	λ_{abs} (10^{-4} ε)[b]	$l\lambda_{fl}$ [c]	Φ[d]	$\lambda_{max}^{(2)}$ [e]	$\Phi\delta_{max}$ [f]
SHS-M1	340 (1.9)	420	0.23 (0.41)	750	14 (32)
1	365 (1.8)	500	0.50 (1.00)	750	63 (76)
SHS-M2	343 (1.4)	464	0.24 (1.00)	740	17 (60)
2	383 (1.5)	545	0.12 (1.00)	750	55 (177)

[a]All measurements were performed in HEPES buffer (30 mM HEPES, 100 mM KCl, pH 7.4) unless otherwise noted. [b]λ_{max} of the one-photon absorption spectra in nm. The numbers in parentheses are molar extinction coefficients in $M^{-1}cm^{-1}$. [c]λ_{max} of the one-photon emission spectra in nm. [d]Fluorescence quantum yield, ± 15 %. The numbers in parentheses are measured in EtOH. [e]λ_{max} of the two-photon excitation spectra in nm. [f]The peak two-photon action cross section in 10^{-50} cm^4s/photon (GM), ± 15%. The numbers in parentheses are measured in EtOH.

Detection of mitochondrial H_2S with SHS-M2 in live cell and tissue

We then tested the utility of SHS-M2 to detect H_2S in the cellular environment. The TPM image of the HeLa cells labeled with SHS-M2 was bright, presumably because of the easy loading, convenient rate of H_2S-induced reduction, and large $\Phi\delta_{max}$ value of the reaction product (Figures 3A-D).

To confirm whether the probes can specifically stain the mitochondria, HeLa cells were stained with SHS-M2 and MitoTracker Red (MTR),[25] a well-known one-photon fluorescent marker for mitochondria. The TPM image of SHS-M2 merged well with the OPM image of MTR (Figure S10). The Pearson's colocalization coefficient (*A*),[26] calculated by using Autoquant X2 software, of SHS-M2 and MTR was 0.85, indicating that this probe exists predominantly in mitochondria. Experiment in astrocytes gave similar result with *A* value of 0.82 (Figure 4). Further, SHS-M2 show low cytotoxicity as determined by using a CCK-8 kit (Figure S11, SI).

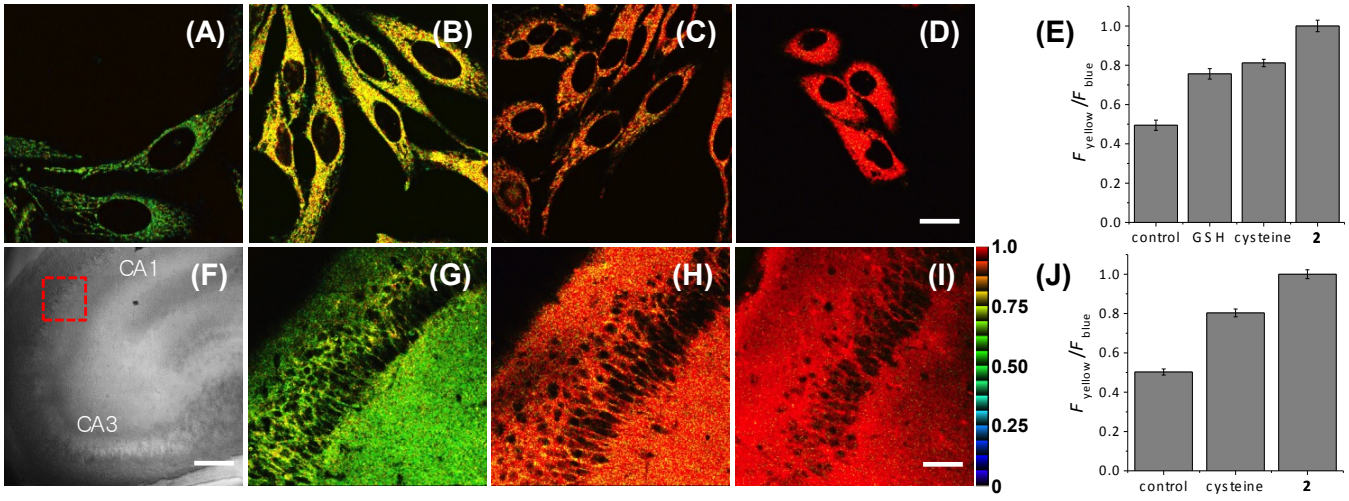

Figure 3. (A-D) Pseudocolored ratiometric TPM images (F_{yellow}/F_{blue}) of HeLa cells incubated with 2 μM (A) SHS-M2 and (D) 2. HeLa cells pretreated with (B) GSH (100 μM) for 30 min and (C) cysteine (100 μM) for 30 min before labeling with SHS-M2. (E) Average F_{yellow}/F_{blue} intensity ratios in (A-D). Images were acquired using 750 nm excitation and emission windows of 425-470 nm (blue) and 525-575 nm (yellow). Cells shown are representative images from replicate experiments (n = 5). (F-I) Images of a rat hippocampal slice stained with 20 μM (G) SHS-M2 and (I) 2 for 1 h. (F) Bright-field images of the CA1 and CA3 regions. Ratiometric TPM images of a fresh rat hippocampal slices that were (G) not treated and (H) pretreated with 1 mM cysteine for 1 h before labeling with SHS-M2. TPM images were acquired at a depth of 120 μm with 40x magnification. (J) Average F_{yellow}/F_{blue} intensity ratios in (G-I). The TP fluorescence emission was collected in two channels (blue = 425-470 nm and yellow = 525-575 nm) upon excitation at 750 nm with a fs-pulses. Scale bars: (D) 20 μm, (F) 300 μm, and (I) 75 μm.

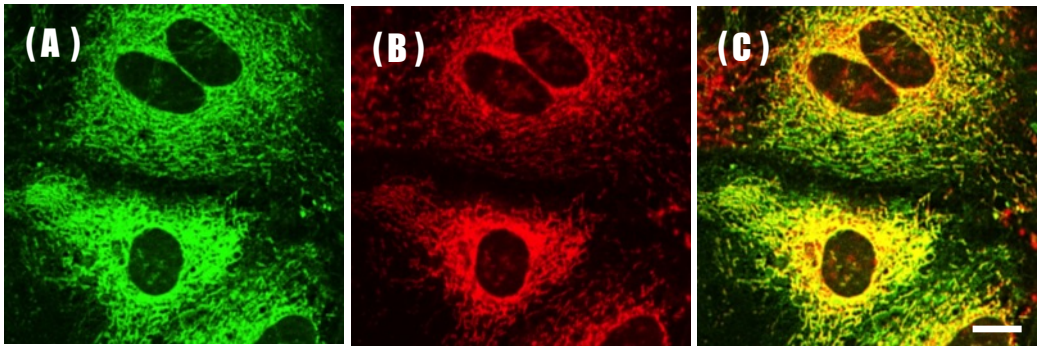

Figure 4. (A) TPM and (B) OPM images of astrocytes colabeled with (A) SHS-M2 and (B) MitoTracker Red FM. (C) Merged image. The wavelengths for TP and OP excitation were 750 and 514 nm, respectively, and the corresponding emissions were collected at 425-575 nm (SHS-M2) and 600-700 nm (Mitotracker Red FM). Scale bar, 30 μm. Cells shown are representative images from replicate experiments (n = 3).

Next, we tested whether SHS-M2 can monitor the changes in mitochondrial H_2S levels in live cells and tissues. Upon TP excitation at 750 nm, the average emission ratios (F_{yellow}/F_{blue}) of HeLa cells labeled with SHS-M2 and **2** were 0.49 and 1.00, respectively (Figures 3A,D,E, and S12, SI). The ratio increased from 0.49 to 0.76 or 0.81, respectively, after addition of GSH or Cys, which are the precursors to H_2S.[5b,27,28] Further, we investigated the utility of SHS-M2 in a fresh rat hippocampal slice. We accumulated 10 TPM images at depths of 90–180 μm to visualize the overall H_2S distribution. They revealed that H_2S are more or less evenly distributed in both the CA1 and CA3 regions (Figure S13 and S14, SI) as well as at different depths. Moreover, the image at a higher magnification clearly shows the H_2S distribution in the individal cells in the CA1 region with an average emission ratio of 0.51 at a depth of 120 μm (Figure 3G,J). The F_{yellow}/F_{blue} ratio increased to 0.80 when the tissue was treated with 1 mM cystein for 50 min (Figure 3H,J). These results confirm that SHS-M2 is clearly capable of monitoring the endogenous H_2S levels in live cells and at > 100 μm depth in living tissues using TPM.

Measurement of H_2S levels in cultured astrocytes with SHS-M2

We next investigated whether SHS-M2 can measure H_2S levels produced by different levels of cystathionine β-synthase (CBS), the major enzyme that catalyzes H_2S production, in astrocytes. It is well established that astrocytes express CBS and produce H_2S in the brain.[2,11,12] We knocked out CBS

from astrocytes using CBS siRNA (5'-CCC AAA AUU UUA CCA GAU AUU CUU U-3'). Astrocytes pretreated with CBS siRNA for 5 days showed significantly reduced CBS mRNA and CBS protein levels as compared to the cells pretreated with non-targeted (NT) siRNA (5'-CCU CGU GCC GUU CCA UCA GGU AGU U-3') (Fig. 5A, B). Moreover, the F_{yellow}/F_{blue} ratio of SHS-M2-labeled astrocytes decreased from 0.66 to 0.56 when pretreated with NT-siRNA and CBS siRNA, respectively, indicating a parallel decrease in the H_2S levels (Fig. 5C, D). This result demonstrates the capability of SHS-M2 to delineate the relationship between the expression levels of CBS and H_2S levels in astrocytes by TPM.

Measurement of endogenous H_2S levels in DJ-1 deficient astrocytes and brain slices

We then utilized SHS-M2 to measure the endogenous H_2S levels in DJ-1 deficient astrocytes and mouse brain slices. DJ-1 is a PD-related gene that has multiple functions. It was reported that DJ-1 exerts anti-inflammatory and anti-oxidant effect in astrocytes.[29-32] Since H_2S also has anti-inflammatory and antioxidant effects,[4,10,11] it was interesting to find out whether DJ-1 regulates H_2S production. Using SHS-M2 as the probe, we found that the F_{yellow}/F_{blue} ratio in DJ-1 knockout (KO) astrocytes decreased to 0.46 from 0.71 measured in wild-type (WT) astrocytes (Fig. 6A, B). This outcome indicates a parallel decrease in the endogenous H_2S levels. Moreover, the CBS mRNA and CBS protein levels were significantly reduced in DJ-1 KO astrocytes compared to WT astrocytes (Fig. 6C, D). Here again, a parallel decrease in the CBS expression levels and endogenous H_2S level is clearly indicated.

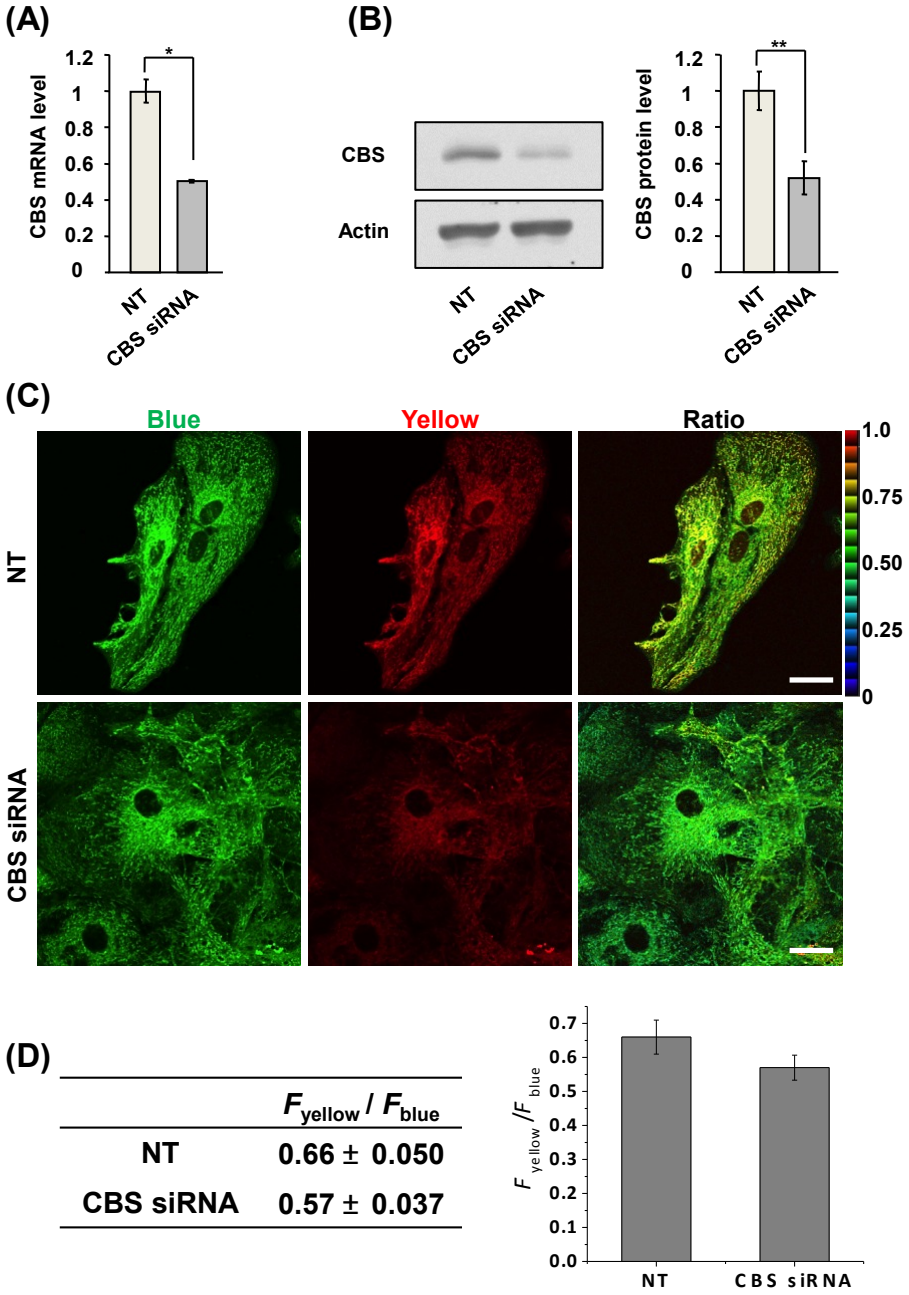

Figure 5. SHS-M2 showed correlation between CBS expression levels and amount of H_2S production. (A, B) Astrocytes prepared from neonate mice brain were treated with CBS-specific siRNA (20 nM) or non-targeted siRNA (NT) for 5 days. CBS mRNA levels (A), and protein levels (B) were analyzed with Q-PCR and Western blot, respectively, and quantified (B). (C) Astrocytes treated with CBS-specific or NT siRNA were stained with 2 μM SHS-M2 for 1 h. Images were acquired using 750 nm excitation and emission windows of 425-470 nm (blue) and 525-575 nm (yellow). (D) Average intensity ratios (F_{yellow}/F_{blue}) in TPM images were calculated as described above. Values in A and B are mean ± SEM of 3 samples, and values in D are mean ± SD of 3 samples. Cells shown in C are representative images from replicate experiments (n = 3). Scale bar in (C), 20 μm.

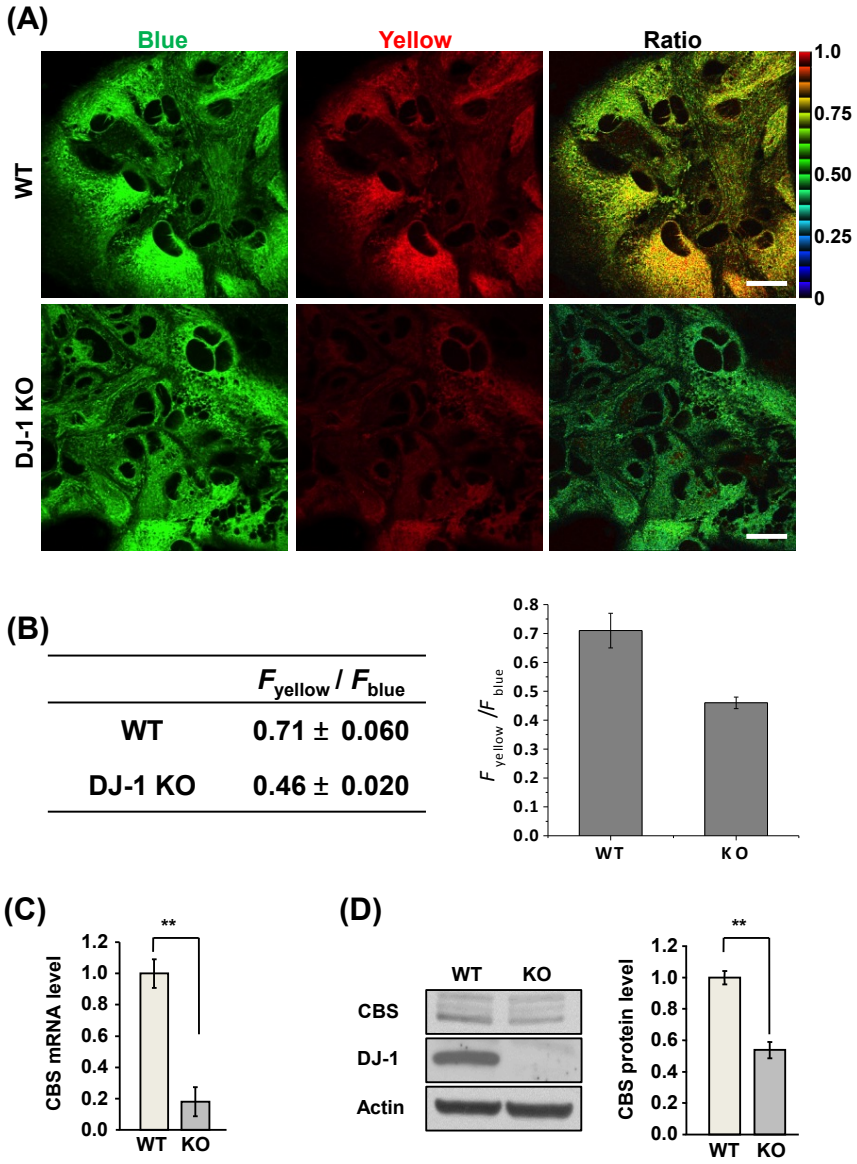

Figure 6. Attenuated H_2S production and expression of CBS in DJ-1 KO astrocytes. (A, B) Astrocytes cultured from WT and DJ-1 KO mice brain were stained with 20 μM SHS-M2 for 1 h. Ratiometric TPM images of astrocytes revealed decreased H_2S production in KO astrocytes compared to WT cells (A). Average F_{yellow}/F_{blue} intensity ratios in TPM images were calculated as described above (B). (C, D) CBS mRNA (C) and protein levels (D) in WR and KO astrocytes were determined with Q-PCR and Western blot, respectively. Values in B are mean ± SD of 3 samples, and values in C and D are mean ± SEM of 3 samples. Scale bar in A, 20 μm.

We further investigated the relationship between CBS expression and H_2S production in WT and DJ-1 KO brain slices. Slices were freshly prepared from WT and KO brain hippocampus, and double-stained with antibodies specific for GFAP (an astrocyte marker) and CBS, respectively. As expected, CBS was

detected in GFAP-positive astrocytes, and its expression was dramatically reduced in DJ-1 KO astrocytes (Fig. 7A). H_2S was also detected in cells having astrocyte-morphology (Fig. 7B), and was significantly reduced in DJ-1 KO slices compared to WT slices (Fig. 7B, C). We then analyzed H_2S production in cortical slices 7 d after slicing to stabilize tissues from slicing stress.[33] The ratiometric images of SHS-M2-labeled tissues showed reduced H_2S levels in DJ-1 KO cortical slices (Fig. 7D, E), as observed in cultured astrocyte (Fig. 6) and freshly prepared slice (Fig. 7B, C). These results indicate that the TPM ratiometric imaging using SHS-M2 as the probe is an effective tool to measure different H_2S levels produced by different CBS expression levels. To the best of our knowledge, this is the first report showing that genetically mutated PD genes can affect H_2S production in PD patients' brain, partially in astrocytes.

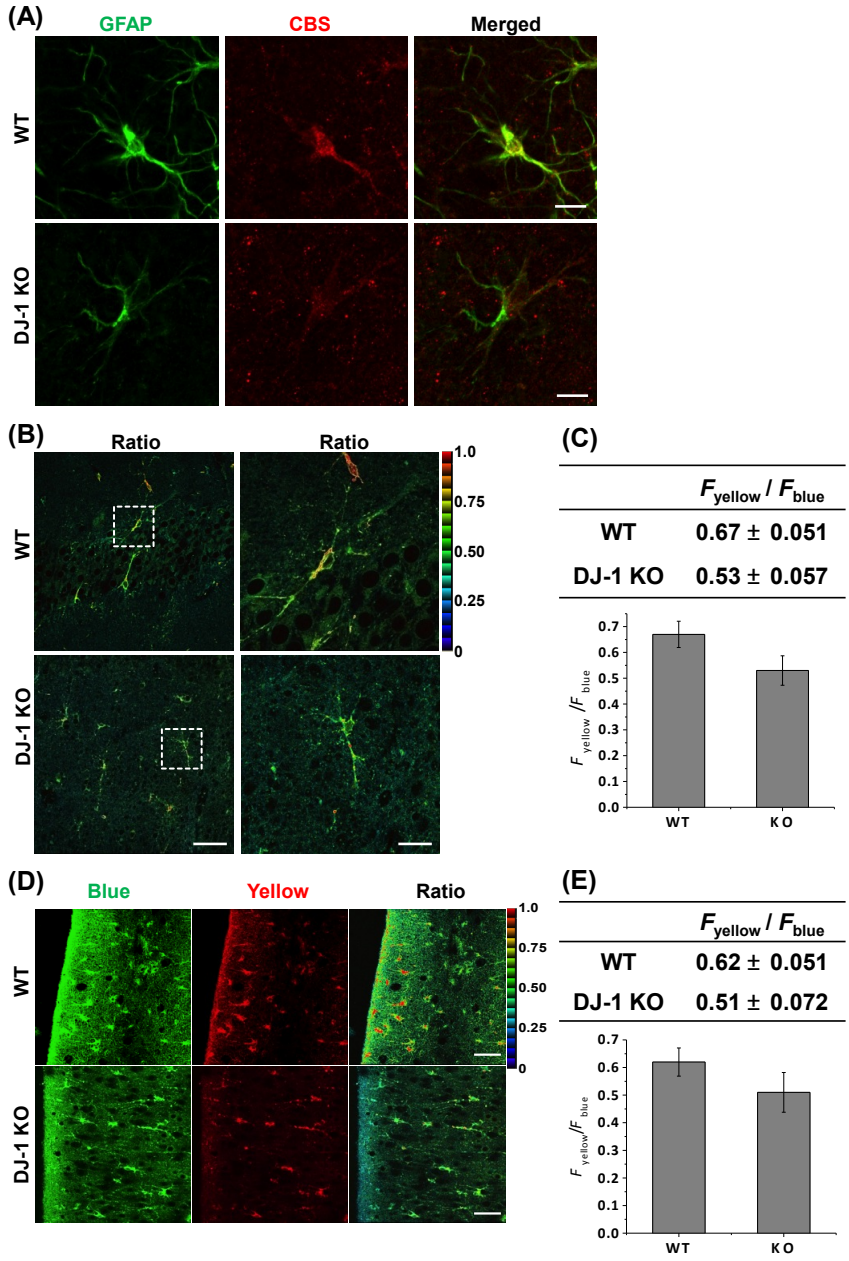

Figure 7. Attenuated CBS expression and H_2S production in astrocytes in DJ-1 KO brain. Brain slices were prepared from WT and DJ-1 KO mice. (A, B, C) Hippocampal slices were acutely prepared and used for GFAP and CBS staining as described in Experimental section (A) or H_2S analysis as above (B, C). Right panels in (B) are higher magnification of boxed areas in left panels in (B). (D, E) Cortical slices were cultured for 7 d after slicing to stabilize tissues from slicing stress, H_2S production was measured. Values in C and E are mean ± SD of 3 samples. Scale bars: 30 μm for A and right panel in B, and 75 μm for left panel in B and D.

Concluding Remarks

In this study, we have developed a new mitochondrial specific and emission ratiometric TP probe for H_2S (SHS-M2), which shows a significant TP cross section, a marked blue-to-yellow emission color

change in response to H_2S, high mitochondrial H_2S selectivity, high photostability, low cytotoxicity, and well-working in biologically relevant pH range. This probe can ratiometrically detect mitochondrial H_2S in the live cells and living tissues for a long period of time by TPM with minimum interference from other biologically relevant species.

In addition, the TPM ratiometric imaging using SHS-M2 is an effective tool to measure different H_2S levels produced by different expression levels of CBS in WT and DJ-1 KO astrocytes and brain slices. These findings demonstrate that H_2S levels decrease in a genetic model of PD. Furthermore, SHS-M2 may find useful applications in biomedical research including PD through the use of TPM.

EXPERIMENTAL SECTION

Spectroscopic measurements. Absorption spectra were recorded on a S-3100 UV-Vis spectrophotometer and fluorescence spectra were obtained with FluoroMate FS-2 fluorescence spectrophotometer with a 1 cm standard quartz cell. The fluorescence quantum yield was determined by using coumarin 307 ($\Phi = 0.95$ in MeOH) as the reference by the literature method.[34]

Measurement of Two-Photon Cross Section. The two-photon cross section (δ) was determined by using femto second (fs) fluorescence measurement technique as described.[35] Dye (1.0×10^{-6} M) was dissolved in 30 mM HEPES buffer (pH = 7.4) and the two-photon induced fluorescence intensity was measured at 720−880 nm by using rhodamine 6G as the reference, whose two-photon property has been well characterized in the literature.[36] The intensities of the two-photon induced fluorescence spectra of the reference and sample emitted at the same excitation wavelength were determined. The TPA cross section was calculated by using $\delta = \delta_r(S_s\Phi_r\phi_r c_r)/(S_r\Phi_s\phi_s c_s)$: where the subscripts *s* and *r* stand for the sample and reference molecules. The intensity of the signal collected by a CCD detector was denoted as *S*. Φ is the fluorescence quantum yield. ϕ is the overall fluorescence collection efficiency of the experimental apparatus. The number density of the molecules in solution was denoted as *c*. δ_r is the TPA cross section of the reference molecule.

Animals. DJ-1 Knock out (KO) mice used in this study were a gift from UJ Kang in Chicago University. DJ-1 KO mice were previously generated by deleting 9.3-kb genomic DNA including the first 5 exons and part of the promoter region of DJ-1 gene (Chen et al., 2005).[37]

Cell Culture. HeLa human cervical carcinoma cells (ATCC, Manassas, VA, USA) were cultured in DMEM (WelGene Inc, Seoul, Korea) supplemented with 10 % FBS (WelGene), penicillin (100 units/ml), and streptomycin (100 μg/mL). Two days before imaging, the cells were passed and plated on glass-bottomed dishes (NEST). All the cells were maintained in a humidified atmosphere of 5/95 (v/v) of CO_2/air at RT. For labeling, the growth medium was removed and replaced with DMEM without FBS. The cells were treated and incubated with 2 μM SHS-M1, **1**, SHS-M2, and **2** at 37 ^oC under 5 % CO_2 for 30 min. The cells were washed three times with phosphate buffered saline (PBS; Gibco) and then imaged after further incubation in colorless serum-free media for 30 min.

Primary astrocytes were cultured from the cortex of DJ-1 KO, or WT mice brains. In brief, cortexes were removed and triturated in DMEM (Invitrogen, Carlsbad, CA, USA) containing 10% FBS (HyClone, Logan, UT, USA), plated in 75 cm^2 T-flasks (0.5 hemisphere/flask), and incubated for 2~3 weeks. Microglia were detached from flasks by mild shaking, filtered through a nylon mesh to remove cell clumps, and cultured in DMEM containing 10% FBS.[38] Astrocytes remaining in the flask were harvested with 0.1% trypsin and cultured in DMEM containing 10% FBS. BV2 murine microglia were cultured in DMEM containing 5% FBS as previously described (Min et al., 2003).[39] For activation of glial cells, cells were treated with 5 ng/ml recombinant murine IFN-(PeproTech, Rocky Hill, NJ, USA).

Preparation and Staining of fresh rat Hippocampal slices. Rat Hippocampal slices were prepared from the hippocampi of 2-weeks-old rat (SD) according to an approved institutional review board protocol. Coronal slices were cut into 400 μm-thick using a vibrating-blade microtome in artificial cerebrospinal fluid (ACSF; 124 mM NaCl, 3 mM KCl, 26 mM $NaHCO_3$, 1.25 mM NaH_2PO_4, 10 mM D-glucose, 2.4 mM $CaCl_2$, and 1.3 mM $MgSO_4$). Slices were incubated with 20 μM SHS-M2 in ACSF bubbled with 95% O_2 and 5% CO_2 for 1 hr 30 min at 37 °C. Slices were then washed three times with

ACSF and transferred to glass-bottomed dishes (NEST) and observed in a spectral confocal multiphoton microscope.

Oragnotypic cortical slice cultures (OCSCs). Cortical slices were prepared according to a previously described protocol with modification.[40] Slices were obtained from postnatal day 7 mice. Briefly, brains were rapidly removed and cortices separated by thin forceps in culture medium. Coronal cortical slices (400 μm thick) were prepared using a McIlwain tissue chopper (Mickle Laboratory Engineering, Goose Green, UK). Slices were placed on membranes (0.4 mm pore size) of inserts (Millipore, cork, Ireland). Each well was filled with slice culture medium (MEM containing 25% [v/v] Hanks' balanced salt solution, 25% [v/v] heat-inactivated horse serum [HyClone], 6.5 mg/mL glucose, 1 mM L-glutamine, 10 U/mL penicillin-G, and 10 mg/mL streptomycin). For stabilization, slices were incubated for 7 days with changing media at day 3 and 5. At day 7, slices were used for experiments.

siRNA transfection. The CBS protein expression in astrocytes was knocked down using CBS-specific siRNA (Genolution Phamaceuticals, Seoul, Korea). CBS specific siRNA sequence was 5'-CCC AAA AUU UUA CCA GAU AUU CUU U-3', and non-targeted siRAN sequence was 5'-CCU CGU GCC GUU CCA UCA GGU AGU U-3'. For siRNA transfection, astrocytes were placed in Opti-MEM (Invitrogen , Carlsbad, CA, USA), and treated with 20 nM siRNA and RNAiMAX transfection reagent. Four hours later, astrocytes were placed in 10% FBS-containg DMEM, and incubated for 5 days. Reduced CBS expression was confirmed using qPCR and Western blot.

Quantitative real-time PCR. CBS mRNA expression was analyzed using Quantitative real-time PCR(qPCR). In brief, total RNA was isolated using RNAzol B (iNtRON, Sungnam, Korea), and cDNA was prepared using Avian Myeloblastosis Virus reverse transcriptase (Promega, Madison, WI, USA) according to the manufacturer's protocol. qPCR was done using 2x KAPA SYBR Fast Master Mix (Kapa Biosystem, Cape Town, South Africa) and RG-6000 real-time amplification instrument (Corbett Research, Sydney, Australia). qPCR primer sets specific for CBS were 5'-CCA TGG CTG TGG CTG TGA A-3'(sense) and 5'-CCA TTT GTC ACT CAG GAA CTT GGA-3'(antisense); For actin, 5'- GCT CTG GCT CCT AGC ACC AT-3'(sense), 5'-GCC ACC GAT CCA CAC AGA GT-3'(antisense). Actin

was used as a reference gene. The threshold cycle values of each of the genes were presented as relative fold induction.

Western blot. Astrocytes were washed with cold PBS and lysed with RIPAa buffer (1% NP-40, 150 mL NaCl, 10 mM Na_2HPO_4, pH 7.2, 0.5% sodium deoxycholate) containing protease inhibitors (2 mM PMSF, 10 μg/L leupeptin, 10 μg/L pepstatin and 0.5 mM $NaVO_3$). Proteins were separated by 10% sodium dodecyl sulfate-polyacrylamide gel electrophoresis (SDS-PAGE) and transferred to nitrocellulose membrane. Membranes were incubated with 5% non-fat milk non-specific antibody binding was blocked with solution, and antibodies specific for CBS (1:1000; Santa Cruz Biotechnology, Santa Cruz, CA, USA), DJ-1 (1:1000; Cell Signaling Technology, Beverly, MA, USA), and b-actin (1:1000; Santa Cruz Biotechnology, Santa Cruz, CA, USA). Membranes were washed, incubated with peroxidase-conjugated secondary antibodies (1:10000; Zymed, San Fransico, CA), visualized by Enhanced ChemiLuminescence (ECL) system (BioNote, Gyeonggi, Korea).

Immunohistochemistry For immunofluorescence staining, slices and/or brain sections were obtained, washed three times in PBS containing 0.2% Triton X-100 (PBST). Non-specific antibody binding was blocked with 1% BSA in PBST. Slices and/or sections were incubated with specific antibodies for GFAP (1:50; Signaling Technology, Beverly, MA, USA) or CBS (1:50; Santa Cruz Biotechnology, Santa Cruz, CA, USA). After washing, slices and/or sections were incubated with secondary antibodies conjugated with Alexa Fluor488- or Alexa Fluor555 (1600 dilution; Invitrogen, Eugene, OR, USA). DAPI (Vector Laboratories, Burlingame, CA) was used to detect nuclei. All samples were analyzed under a confocal microscope (Carl Zeiss, Germany) with 63× oil immersion objectives.

Two-Photon Fluorescence Microscopy. Two-photon fluorescence microscopy images of SHS-M1, **1**, SHS-M2, and **2**-labeled cells and tissues were obtained with spectral confocal and multiphoton microscopes (Leica TCS SP8 MP) with ×10 dry, ×40 oil, ×63 oil, and ×100 oil objectives, numerical aperture (NA) = 0.30, 0.30, 1.40, and 1.30, respectively. The two-photon fluorescence microscopy images were obtained with a DMI6000B Microscope (Leica) by exciting the probes with a mode-locked

titanium-sapphire laser source (MaiTai spectra physics, 80 MHz, 100 fs) set at wavelength 750 nm and output power 2710 mW, which corresponded to approximately 10 mW average power in the focal plane. To obtain images at 425~575 nm range, internal PMTs were used to collect the signals in an 8 bit unsigned 512 × 512 and 1024 × 1024 pixels at 400 and 200 Hz scan speed, respectively. Ratiometric image processing and analysis was carried out using MetaMorph software.

ASSOCIATED CONTENT

Supporting Information. Synthesis, additional methods, figures (Figure S1-S20) and table S1. This material is available free of charge via the Internet at http://pubs.acs.org.

AUTHOR INFORMATION

Corresponding Authors

kimhm@ajou.ac.kr; chobr@korea.ac.kr; ehjoe@ajou.ac.kr

Author Contributions

‡These authors contributed equally.

ACKNOWLEDGMENT

National Research Foundation (NRF) grants funded by the Korean Government (No. 20120008780 and 2012007850), Priority Research Centers Program through the NRF (20120006687 and 20120005860), and NRF through the Chronic Inflammatory Disease Research Center (CIDRC) at Ajou University (NRF-2012R1A5A2051429).

REFERENCES

(1) Kimura, H. *Amino acids* **2011**, *41*, 113.

(2) Abe, K.; Kimura, H. *J. Neurosci*. **1996**, *16*, 1066.

(3) Kabil, O.; Banerjee, R. *J. Biol. Chem*. **2010**, *285*, 21903.

(4) Zanardo, R. C.; Brancaleone, V.; Distrutti, E.; Fiorucci, S.; Cirino, G.; Wallace, J. L. *FASEB*. **2006**, *20*, 2118.

(5) (a) Kimura, Y.; Goto, Y.; Kimura, H. *Antioxid. Redox Signal*. **2010**, *12*, 1. (b) Shibuya, N.; Tanaka, M.; Yoshida, M.; Ogasawara, Y.; Togawa, T.; Ishii, K.; Kimura, H. *Antioxid. Redox Signal*. **2009**, *11*, 703.

(6) (a) Mari, M.; Morales, A.; Colell, A.; Garcia-Ruiz, C.; Fernandez-Checa, J. C. *Antioxid. Redox Signal*. **2009**, *11*, 2685. (b) Cheng, W. Y.; Tong, H.; Miller, E. W.; Chang, C. J.; Remington, J.; Zucker, R. M.; Bromberg, P. A.; Samet, J. M.; Hofer, T. P. *Environ. Health Perspect*. **2010**, *118*, 902.

(7) (a) Pun, P. B.; Lu, J.; Kan, E. M.; Moochhala, S. *Mitochondrion* **2010**, *10*, 83. (b) Fu, M.; Zhang, W.; Wu, L.; Yang, G.; Li, H.; Wang, R. *Proc. Natl. Acad. Sci. U. S. A*. **2012**, *109*, 2943.

(8) Warenycia, M. W.; Goodwin, L. R.; Benishin, C. G.; Reiffenstein, R. J.; Francom, D. M.; Taylor, J. D.; Dieken, F. P. *Biochem. Pharmacol*. **1989**, *38*, 973.

(9) Goodwin, L. R.; Francom, D.; Dieken, F. P.; Taylor, J. D.; Warenycia, M. W.; Reiffenstein, R. J.; Dowling, G. *J. Anal. Toxicol*. **1989**, *13*, 105.

(10) Hu, L. F.; Lu, M.; Tiong, C. X.; Dawe, G. S.; Hu, G.; Bian, J. S. *Aging Cell* **2010**, *9*, 135.

(11) Lee, M.; Schwab, C.; Yu, S.; McGeer, E.; McGeer, P. L. *Neurobiol. Aging* **2009**, *30*, 1523.

(12) Eto, K.; Asada, T.; Arima, K.; Makifuchi, T.; Kimura, H. *Biochem. Biophys. Res. Commun*. **2002**, *293*, 1485.

(13) (a) Lippert, A. R.; New, E. J.; Chang, C. J. *J. Am. Chem. Soc.* **2011**, *133*, 10078. (b) Peng, H.; Cheng, Y.; Dai, C.; King, A. L.; Predmore, B. L.; Lefer, D. J.; Wang, B. *Angew. Chem. Int. Ed.* **2011**, *50*, 9672. (c) Chen, S.; Chen, Z.; Ren, W.; Ai, H.-W. *J. Am. Chem. Soc.* **2012**, *134*, 9589.

(14) Sasakura, K.; Hanaoka, K.; Shibuya, N.; Mikami, Y.; Kimura, Y.; Komatsu, T.; Ueno, T.; Terai, T.; Kimura, H.; Nagano, T. *J. Am. Chem. Soc.* **2011**, *133*, 18003.

(15) (a) Qian, Y.; Karpus, J.; Kabil, O.; Zhang, S. Y.; Zhu, H. L.; Banerjee, R.; Zhao, J.; He, C. *Nat. Commun.* **2011**, *2*, 495. (b) Liu, C.; Pan, J.; Li, S.; Zhao, Y.; Wu, L. Y.; Berkman, C. E.; Whorton, A. R.; Xian, M. *Angew. Chem. Int. Ed.* **2011**, *50*, 10327.

(16) Chen, Y.; Zhu, C.; Yang, Z.; Chen, J.; He, Y.; Jiao, Y.; He, W.; Qiu, L.; Cen, J.; Guo, Z. *Angew. Chem. Int. Ed.* **2013**, *52*, 1688.

(17) (a) Helmchen, F.; Denk, W. *Nat. Methods* **2005**, *2*, 932. (b) Zipfel, W. R.; Williams, R. M.; Webb, W. W. *Nat. Biotechnol.* **2003**, *21*, 1369.

(18) (a) Kim, H. M.; Cho, B. R. *Accounts Chem. Res.* **2009**, *42*, 863. (b) Kim, H. M.; Cho, B. R. *Chem. Asian J.* **2011**, *6*, 58. (c) Sumalekshmy, C.; Fahrmi, C. J. *Chem. Mat.* **2011**, *23*, 483. (d) S. Yao, K. D. Belfield, *Eur. J. Org. Chem.* **2012**, 3199.

(19) (a) Li, L.; Ge, J.; Wu, H.; Xu, Q. H.; Yao, S. Q. *J. Am. Chem. Soc.* **2012**, *134*, 12157. (b) Rao, A. S.; Kim, D.; Nam, H.; Jo, H.; Kim, K. H.; Ban, C.; Ahn, K. H. *Chem. Commun.* **2012**, *48*, 3206. (c) Dong, X.; Yang, Y.; Sun, J.; Liu, Z.; Liu, B. F. *Chem. Commun.* **2009**, 3883.

(20) (a) Masanta, G.; Heo, C. H.; Lim, C. S.; Bae, S. K.; Cho, B. R.; Kim, H. M. *Chem. Commun.* **2012**, *48*, 3518. (b) Lim, C. S.; Masanta, G.; Kim, H. J.; Han, J. H.; Kim, H. M.; Cho, B. R. *J. Am. Chem. Soc.* **2011**, *133*, 11132. (c) Masanta, G.; Lim, C. S.; Kim, H. J.; Han, J. H.; Kim, H. M.; Cho, B. R. *J. Am. Chem. Soc.* **2011**, *133*, 5698.

(21) R. J. Griffin, El. Evers, R. Davison, A. E. Gibson, D. Layton and W. J. Irwin, *J. Chem. Soc., Perkin Trans. 1*, **1996**, 1205.

(22) pK_1 (6.96) and pK_2 (12.90) values of H_2S predict that H_2S and HS^- are the predominant sulfide species in aqueous solution regardless of whether H_2S, NaHS, or Na_2S is used.

(23) Makarov, N. S.; Drobizhev, M.; Rebane, A. *Opt. Express* **2008**, *16*, 4029.

(24) Kim, H. M.; Cho, B. R. *Chem. Commun.* **2009**, 153.

(25) A Guide to Fluorescent Probes and Labeling Technologies, 10th ed. (Ed.: R. P. Haugland), Molecular Probes, Eugene, OR, **2005**.

(26) Manders, E. M.; Stap, J.; Brakenhoff, G. J.; van Driel, R.; Aten, J. A. *J. Cell Sci.* **1992**, *103 (Pt 3)*, 857.

(27) (a) Singh, S.; Padovani, D.; Leslie, R. A.; Chiku, T.; Banerjee, R. *J. Biol. Chem.* **2009**, *284*, 22457. (b) Hosoki, R.; Matsuki, N.; Kimura, H. *Biochem. Biophys. Res. Commun.* **1997**, *237*, 527.

(28) (a) Griffith, O. W.; Bridges, R. J.; Meister, A. Proc. *Natl. Acad. Sci. U. S. A.* **1978**, *75*, 5405. (b) Kumar, T. R.; Wiseman, A. L.; Kala, G.; Kala, S. V.; Matzuk, M. M.; Lieberman, M. W. *Endocrinology* **2000**, *141*, 4270. (c) Lieberman, M. W.; Wiseman, A. L.; Shi, Z. Z.; Carter, B. Z.; Barrios, R.; Ou, C. N.; Chevez-Barrios, P.; Wang, Y.; Habib, G. M.; Goodman, J. C.; Huang, S. L.; Lebovitz, R. M.; Matzuk, M. M. *Proc. Natl. Acad. Sci. U. S. A.* **1996**, *93*, 7923.

(29) Waak, J.; Weber, S. S.; Waldenmaier, A.; Gorner, K.; Alunni-Fabbroni, M.; Schell, H.; Vogt-Weisenhorn, D.; Pham, T. T.; Reumers, V.; Baekelandt, V.; Wurst, W.; Kahle, P. J. *FASEB.* **2009**, *23*, 2478.

(30) Cornejo Castro, E. M.; Waak, J.; Weber, S. S.; Fiesel, F. C.; Oberhettinger, P.; Schutz, M.; Autenrieth, I. B.; Springer, W.; Kahle, P. J. *J. Neural Transm.* **2010**, *117*, 599.

(31) Junn, E.; Taniguchi, H.; Jeong, B. S.; Zhao, X.; Ichijo, H.; Mouradian, M. M. Proc. *Natl. Acad. Sci. U. S. A.* **2005**, *102*, 9691.

(32) Ren, H.; Fu, K.; Wang, D.; Mu, C.; Wang, G. *J. Biol. Chem.* **2011**, *286*, 35308.

(33) Huuskonen, J.; Suuronen, T.; Miettinen, R.; van Groen, T.; Salminen, A. *J. Neuroinflamm.* **2005**, *2*, 25.

(34) J. N. Demas, G. A. Crosby, *J. Phys. Chem.***1971**, *75*, 991.

(35) Lee, S. K.; Yang, W. J.; Choi, J. J.; Kim, C. H.; Jeon, S. J.; Cho, B. R. *Org. Lett.* **2005**, *7*, 323.

(36) Makarov, N. S.; Drobizhev, M.; Rebane, A. *Opt. Express* **2008**, *16*, 4029.

(37) Chen, L.; Cagniard, B.; Mathews, T.; Jones, S.; Koh, H. C.; Ding, Y.; Carvey, P. M.; Ling, Z.; Kang, U. J.; Zhuang, X. *J. Biol. Chem.* **2005**, *280*, 21418.

(38) Pyo, H.; Jou, I.; Jung, S.; Hong, S.; Joe, E. H. *Neuroreport* **1998**, *9*, 871.

(39) Min, K. J.; Jou, I.; Joe, E. *Biochem. Biophys. Res. Commun.* **2003**, *312*, 969.

(40) Stoppini, L.; Buchs, P. A.; Muller, D. *J. Neurosci. Methods* **1991**, *37*, 173.

SYNOPSIS TOC